



Author(s) Lohan, Elena Simona; Burian, Adina; Renfors, Markku

Title Low-complexity unambiguous acquisition methods for BOC-modulated CDMA signals

Citation Lohan, Elena Simona; Burian, Adina; Renfors, Markku 2008. Low-complexity unambiguous acquisition methods for BOC-modulated CDMA signals. International journal of satellite communications vol. 26, num. 6, 503-522.

Year 2008

DOI <http://dx.doi.org/10.1002/sat.922>

Version Post-print

URN <http://URN.fi/URN:NBN:fi:ty-201407071338>

Copyright This is the accepted version of the following article: Lohan, E. S., Burian, A. and Renfors, M. (2008), Low-complexity unambiguous acquisition methods for BOC-modulated CDMA signals. Int. J. Satell. Commun. Network., 26: 503–522., which has been published in final form at <http://onlinelibrary.wiley.com/doi/10.1002/sat.922/abstract>.

All material supplied via TUT DPub is protected by copyright and other intellectual property rights, and duplication or sale of all or part of any of the repository collections is not permitted, except that material may be duplicated by you for your research use or educational purposes in electronic or print form. You must obtain permission for any other use. Electronic or print copies may not be offered, whether for sale or otherwise to anyone who is not an authorized user.

Low-complexity unambiguous acquisition methods for BOC-modulated CDMA signals

Elena Simona Lohan, Adina Burian, and Markku Renfors

Institute of Communications Engineering, Tampere University of Technology
P.O. Box 553, FIN-33101, Finland, Tel: +358 3 3115 3915, Fax: +358 3 3115 3808
elena-simona.lohan@tut.fi, adina.burian@tut.fi, markku.renfors@tut.fi

Abstract

The new M-code signals of GPS and the signals proposed for the future Galileo systems are of split-spectrum type, where the pseudorandom (PRN) code is multiplied with rectangular sub-carriers in one or several stages. Sine and Cosine Binary-Offset-Carrier (BOC) modulations are examples of modulations which split the signal spectrum and create ambiguities in the envelope of the Autocorrelation Function (ACF) of the modulated signals. Thus, the acquisition of split-spectrum signals, based on the ambiguous ACF, poses some challenges, which might be overcome at the expense of higher complexity (e.g., by decreasing the step of searching the timing hypotheses). Recently, two techniques which deal with the ambiguities of the ACF have been proposed, and they were referred to as 'sideband techniques' (by Betz, Fishman & al.) or 'BPSK-like' techniques (by Martin, Heiries & al.), since they use sideband correlation channels and the obtained ACF looks similar to the ACF of a BPSK-modulated PRN code. These techniques allow the use of a higher search step compared with the ambiguous ACF situation. However, both these techniques use sideband-selection filters and modified reference PRN codes at the receivers, which affect the implementational complexity. Moreover, the 'BPSK-like' techniques have been so far studied for even BOC-modulation orders (i.e., integer ratio between the sub-carrier frequency and the chip rate) and they fail to work for odd BOC-modulation orders (or, equivalently, for split-spectrum signals with significant zero-frequency content). We propose here three reduced-complexity methods which remove the ambiguities of the ACF of the split-spectrum signals and work for both even and odd BOC-modulation orders. Two of the proposed methods are extensions of the previously mentioned techniques, and the third one is introduced by the authors and called the Unsuppressed Adjacent Lobes (UAL) technique. We argue

This work has been carried out in the project "Advanced Techniques for Personal Navigation (ATENA)" funded by the Finnish Funding Agency for Technology and Innovation (Tekes). This work has also been supported by the Academy of Finland.

via theoretical analysis the choice of the parameters of the proposed methods and we compare the alternative methods in terms of complexity and performance.

Index Terms

Binary-Offset-Carrier (BOC) modulation, BPSK-like methods, Code Acquisition, Double-Sideband (SB) Correlator, Galileo, Single-SB Correlator, Unambiguous BOC techniques.

I. BACKGROUND AND MOTIVATION

Over the past two decades, satellites in orbit around the earth have become absolutely critical to navigation applications. New services are emerging based on positioning information, such as the location-based applications (e.g., asset tracking, personal security, location-based billing), high-precision guidance in transportation (air, maritime or land), safety-of-life applications, emergency call positioning, etc.[1], [2], [3].

The signals selected for the main navigation systems nowadays, namely Navstar GPS (military-operated US system) and the upcoming Galileo (civil-operated European system), are spread-spectrum signals, modulated either via binary/quaternary phase shift keying (BPSK/QPSK) or by some variants of the so-called Binary-Offset-Carrier (BOC) modulation, e.g., sine BOC (SinBOC), cosine BOC (CosBOC), or alternate BOC (AltBOC) [3], [4], [5], [6], [7], [8], [9], [10]. The BOC modulation splits the signal spectrum into two symmetrical components around the carrier frequency, by multiplying the pseudorandom (PRN) code with a rectangular sub-carrier [4]. The typical notation for BOC modulation is $\text{BOC}(m, n)$, where m and n are two positive indices (not necessarily integers, but with integer ratio $2m/n$), satisfying the relationships $m = f_{sc}/f_{ref}$ and $n = f_c/f_{ref}$, respectively, where f_{sc} is the sub-carrier frequency, f_c is the chip rate, and f_{ref} is a reference frequency (typically, $f_{ref} = 1.023$ MHz) [4], [6]. From the baseband point of view, the signal is fully characterized by twice the ratio between the sub-carrier frequency and the chip rate,

denoted in what follows by BOC-modulation order N_{BOC} [11], [12]

$$N_{BOC} \triangleq \frac{2f_{sc}}{f_c} = \frac{T_c}{T_{sc}} = \frac{2m}{n} \quad (1)$$

Above, T_c is the chip duration and $T_{sc} = \frac{1}{2f_{sc}}$ is the sub-carrier pulse duration. The spectrum splitting due to BOC modulation triggers new challenges in the delay-frequency acquisition process. On one hand, BOC-modulated signals have a narrower main lobe of their Autocorrelation Function (ACF), which may allow a better accuracy in the delay tracking process (however, we might have to deal with the lock-to-a-false-peak problem). On the other hand, the acquisition process becomes more complex, due to the ambiguities (i.e., additional peaks within ± 1 chip interval around the maximum peak) in the envelope of the ACF, which impose a large number of timing hypotheses for accurate detection of the signal [13]. This translates to the fact that the step $(\Delta t)_{bin}$ of searching the time bins in the acquisition process should be sufficiently small, in order to be able to detect the main lobe of the ACF (i.e., we need a higher number of timing hypotheses in order to search a given time-uncertainty window compared to BPSK case) [13]. Thus, the acquisition becomes more computationally expensive, the computational load being inversely proportional with the time-bin size (or step) $(\Delta t)_{bin}$ [13]. This step should be, typically, about a quarter or (at most) half of the width of the main lobe. This width, in its turn, is dependent on the modulation order N_{BOC} . For example, for CosBOC(15,2.5) case, proposed for Galileo Publicly Regulated Signals (PRS) [14], $N_{BOC} = 12$ and the width of the main lobe of the envelope of the ACF is about 0.08 chips (therefore, a step smaller than 0.04 chips should be used for accurate acquisition, which will increase tremendously the computational time, compared with the situation when BPSK modulation where steps of 0.5 chips are typically used).

Recently, two techniques have been proposed in order to deal with the ambiguities of the envelope of the ACF, and thus to allow the use of a higher step in the acquisition process. These techniques are: the 'BPSK-like techniques', proposed by Martin, Heiries & al. [15], [16] and the

'Sideband (SB) techniques', proposed by Betz, Fishman & al. [5], [13], [17], and analyzed also in [18], [19]. However, both these techniques use SB-selection filters and modified reference PRN codes at the receivers, which affect the implementational complexity. Moreover, both methods have been so far tested for SinBOC-modulation and for even BOC-modulation orders only. While the second method (of Betz, Fishman & al.) is still working for CosBOC cases and for odd BOC-modulation orders, as it will be shown in our paper, the first method (of Martin, Heiries & al.) fails to function for odd BOC-modulation orders, due to the high spectral content of the modulated signal around the carrier frequency.

The purpose of our paper is two-fold: first, to introduce a theoretical framework in order to describe the techniques which deals with the above-mentioned ACF ambiguities¹. Second, our paper proposes three new unambiguous acquisition techniques which reduce the implementational complexity (compared with the existing unambiguous acquisition techniques) at the expense of a slight deterioration of performance. These three new low-complexity techniques are: the modified Betz&Fishman method, the modified Betz&Heiries method, and the Unsuppressed Adjacent Lobes (UAL) method. All these techniques can be used either in single-SB or in dual-SB approach.

The rest of the paper is organized as follows. Section II presents the existing unambiguous-acquisition techniques, namely Betz, Fishman & al. methods and Martin, Heiries & al. methods. Section III describes the architecture of the proposed low-complexity techniques. Section IV describes the theoretical framework for the unambiguous-acquisition techniques and justifies the choice of the parameters in the architecture of Section III. Sections V and VI compare the alternative algorithms in terms of performance and implementational complexity, respectively. Section VII presents the conclusions.

¹ These techniques will be, from now on, referred to as "unambiguous acquisition techniques".

II. EXISTING UNAMBIGUOUS-ACQUISITION TECHNIQUES

The following two families of techniques have been proposed in the literature so far in order to cope with the ambiguities of the envelope of the ACF of a BOC-modulated pseudorandom sequence:

- Single- and dual-SB methods, proposed by Betz & al. [5], [17], and by Fishman & al. [13], and denoted in what follows by **B&F methods** (after the initials of the first authors). The block diagram of the dual-SB B&F method is shown in Fig. 1. The single-SB B&F method keeps only one of the bands (either upper or lower) when forming the decision statistic. Both the received signal and the reference code (assumed to be real) are filtered and their upper (or lower) bands are correlated, then added non-coherently. Therefore, the single-sideband B&F method needs one complex SB-selection filter for the real code and two complex SB-selection filters for the received signal (which is complex). The dual-SB B&F method requires twice the number of single-SB filters. The number of filters for each method will be summarized in Section VI (see Table I). The single-SB B&F method suffers of higher non-coherent correlation losses than the dual-SB B&F method [13].
- BPSK-like techniques, proposed by Martin & al. [15] and by Heiries & al. [16], and denoted in what follows by **M&H methods**. The main difference compared with B&F method is the fact that only one real filter is used for the complex received signal (this is equivalent to two real filters for real signals, one for in-phase component and one for the quadrature component). The filter bandwidth includes the two principal lobes of the spectrum and all the secondary lobes between the principal ones (if any), as shown in the block diagram of Fig. 2. The number of filters is the same for single-SB and double-SB schemes. Another difference is that, the reference code is not the filtered BOC-modulated code sequence, but the BPSK-modulated code, held at sub-sample rate (hold factor $N_s N_{BOC}$, where N_s

is the number of samples per BOC interval) and shifted with a quantity equal to the sub-carrier frequency $\pm f_{sc}$, or equivalently with $\pm \frac{N_{BOC}}{2} f_c$ (the \pm sign stands for upper or lower sideband processing). The BPSK-like techniques can be, again, either single or dual SB, according to whether both correlation channels are used (and combined non-coherently) or only one correlation channel is used. The M&H methods have only been tested so far for SinBOC modulations of even N_{BOC} order. Simulation results show that they fail to work for odd N_{BOC} orders, due to an improper shifting factor (the shift factor is defined here as the term $\pm \frac{N_{BOC}}{2}$ which multiplies the chip rate f_c), as illustrated in Fig. 3 for dual-SB processing (the same holds for single SB).

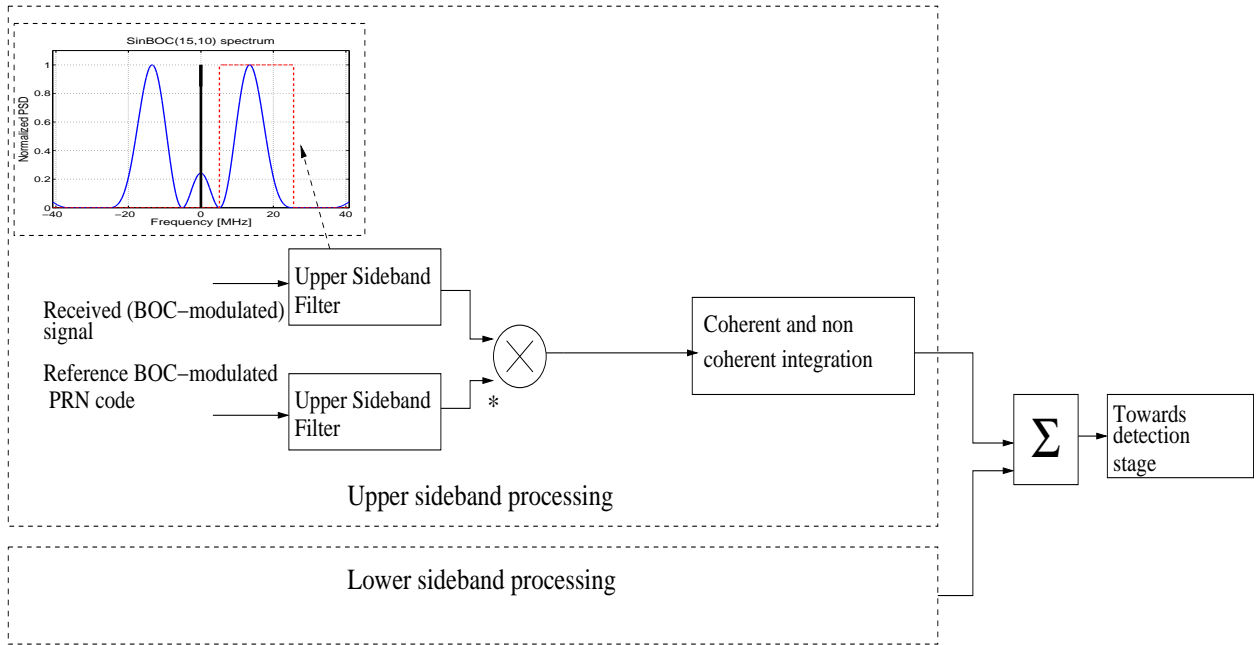


Fig. 1. Block diagram of B&F acquisition method, dual SB processing. The spectrum is shown for SinBOC(15,10) case, i.e., odd modulation order $N_{BOC} = 3$.

III. PROPOSED UNAMBIGUOUS ACQUISITION TECHNIQUES

The complexity of an unambiguous acquisition technique depends, on one hand, on the number of filters used in processing the data, and, on the other hand, on the correlation part. The

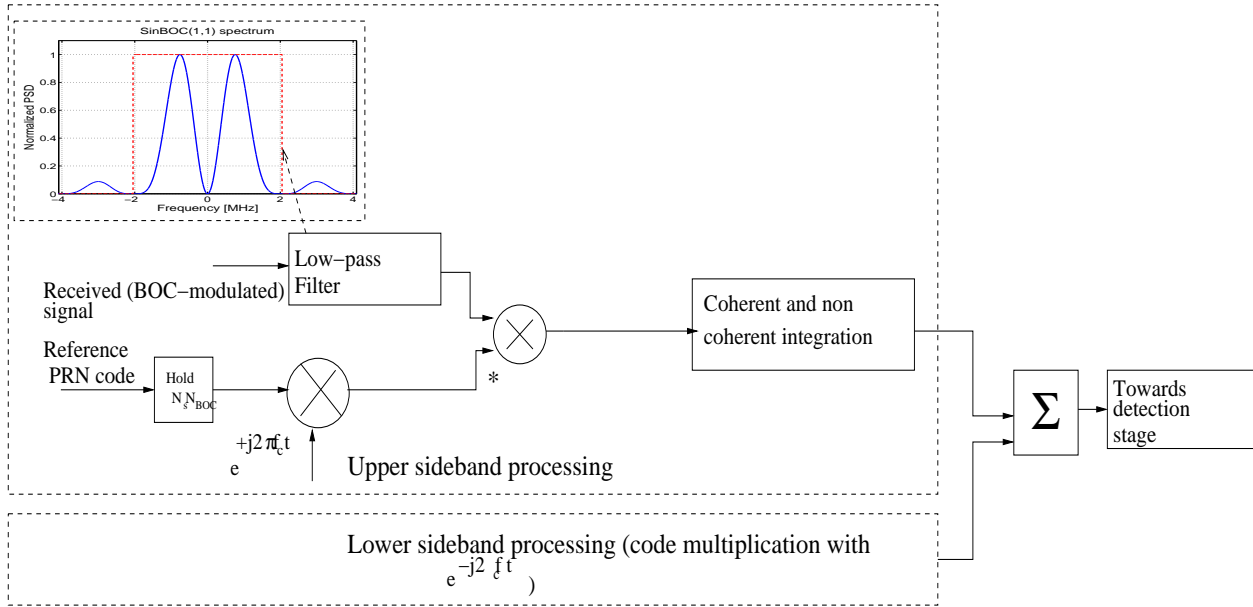


Fig. 2. Block diagram of M&H method, dual SB processing. Here the spectrum is shown for SinBOC(1,1) case, i.e., even modulation order $N_{BOC} = 2$.

correlation part can be implemented either in time domain or in frequency domain [20]. The time-domain correlations are typically preferred for low-cost receiver architectures. The complexity of a time-domain-based correlation can be tremendously decreased if the reference code is kept as a sequence of ± 1 (real or complex numbers), since the complex multiplications will be replaced in this case by simple additions and sign inversions, as shown in [20].

Our proposed methods try to reduce the complexity of the correlation part, and possibly, also the number of used filters. Therefore, the connecting factor of the proposed methods is that the reference code will be the BPSK-modulated chip sequence (and not the upper or lower part of the BOC-modulated chip sequence as in B&F and M&H methods). Three possible structures are proposed and compared (the generic architecture is shown in Fig. 4):

- **Modified B&F methods²**: The main upper or lower lobes of the received signal are first shifted around zero frequency, with a shift factor which is dependent on the BOC-modulation

² The plural refers to both dual and single-SB variants.

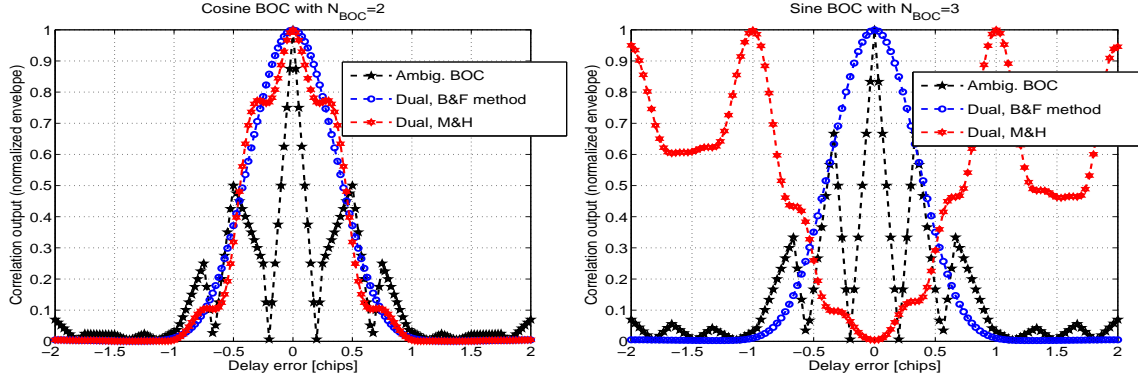


Fig. 3. Illustration of the envelope of the correlation functions after dual -band processing with B&F and M&H methods, for even (left plots) and odd (right plots) BOC-modulation orders. The ambiguous BOC shape is also shown as a reference.

order and which will be optimally computed in Section IV. Then, the main lobes are selected via SB selection filters (either both are selected, if dual-SB processing is desired, or only one of them is selected, if single-SB processing is used). The reference code is the BPSK-modulated PRN sequence of ± 1 .

- Modified M&H methods:** The same processing as for the modified B&F methods is used, with the difference that, instead of selecting only the main lobes (upper or lower), we select both the main lobes and everything between them. The differences with the original M&H method (described in Section II) are that the shift is applied to the received signal (and not to the code) and that, for dual-SB processing, the number of needed filters doubles compared to the dual M&H approach, because the shift factor is applied before filtering and it is different for upper and for lower SB processing, respectively. Thus, the reference code is again the BPSK-modulated PRN sequence, which will be beneficial in reducing the complexity of the correlation part.
- Unsuppressed Adjacent Lobes (UAL) methods:** We use similar processing as for the modified B&F and modified M&H methods, but we remove completely the filtering part. Hence, the lobes which are adjacent to the main lobes are fully unsuppressed and may

affect the performance of the acquisition block. The advantage is that no extra-filters are needed, which will reduce the complexity of the receiver part. The reference code is still the BPSK-modulated PRN sequence of ± 1 .

The generic block diagram of the above proposed techniques is given in Fig. 4. We use

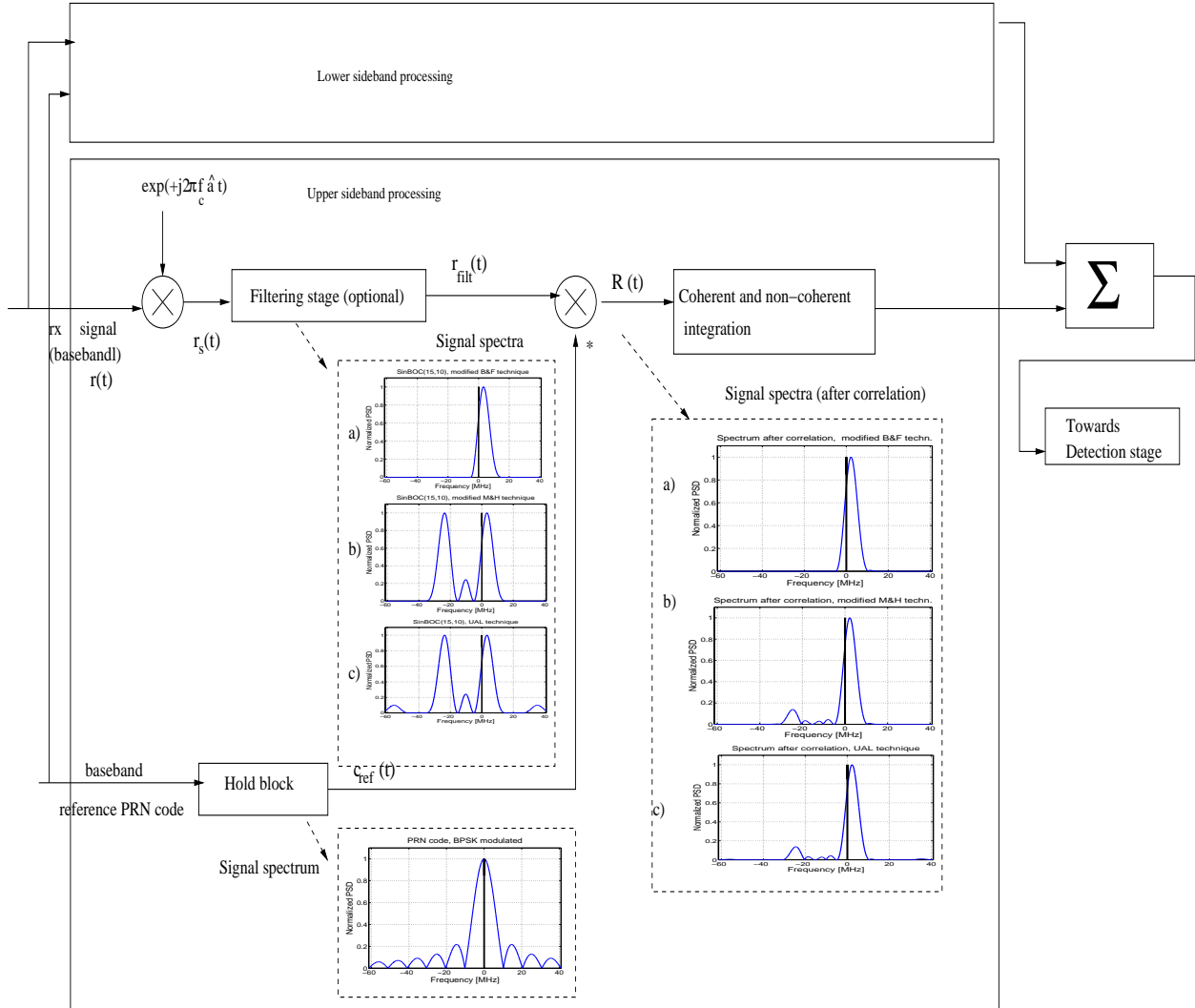


Fig. 4. Block diagram of low-complexity acquisition unit for unambiguous BOC processing: a) modified B&F method, b) modified M&H method, c) UAL method. Here the spectra are shown for SinBOC(15,10) case (i.e., odd modulation order).

the baseband model in what follows, which means that the carrier frequency has been removed beforehand. As seen in Fig. 4, the received signal (BOC-modulated) is shifted up or down, such

that one of the main lobes of the BOC spectrum moves towards zero frequency. The shifting is done via multiplication with an exponential $\exp(\pm j2\pi\hat{a}f_c t)$. We remark the presence of the shift factor \hat{a} in the exponential, which will be determined optimally, via theoretical analysis in Section IV, according to N_{BOC} . The filtering stage is optional, according whether the modified B&F, the modified M&H, or the UAL methods are used (the spectrum for each case is illustrated in Fig. 4 for a SinBOC with $N_{BOC} = 3$ modulation).

The hold block applied to the reference input PRN code is needed in order to preserve the rates (because the reference code is at chip level, while the received signal is at sample level). The hold factor is equal to $N_s N_{BOC}$ for SinBOC modulation, as it will be explained in Section IV. Either a single sideband or both sidebands can be used, similar with B&F and M&H methods. The shapes of the normalized envelope of the ACF after the unambiguous processing with the proposed techniques is shown in Fig. 5, for two representative examples (CosBOC with even N_{BOC} and dual-SB processing and SinBOC with odd N_{BOC} and single-SB processing). Based on various other shapes, which were not included here for reasons of compactness, we noticed that the shapes of the ACF curves depend only on whether N_{BOC} was odd or even and whether the processing was via single SB or via dual SB (they do not depend on the type of the modulation, i.e. SinBOC or CosBOC).

For the modified M&H and UAL technique, some small residual peaks can be observed, due to the fact that there is some interference from the neighbor bands into the main lobe of the signal spectrum (since they are not filtered out completely, as it is the case for the modified B&F). These residual peaks are slightly higher for odd N_{BOC} than for even N_{BOC} . For single-SB processing, the width of the main lobe of the ACF is slightly wider than for dual-SB processing. On the other hand, as expected and as it will be noticed also from simulations, the correlation losses are higher for single SB than for dual SB.

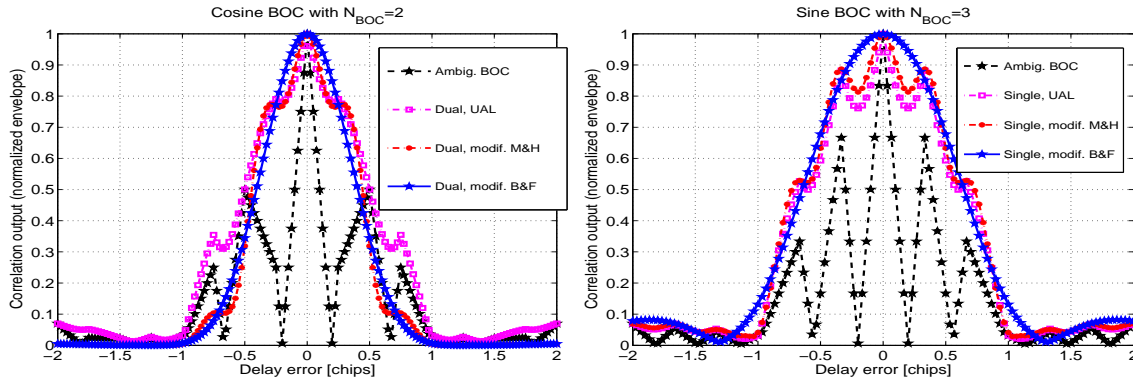


Fig. 5. Illustration of the envelope of the correlation functions after processing with the proposed techniques (modified B&F, modified M&H, and UAL methods). Left figure: even BOC-modulation order and dual-SB processing. Right figure: odd BOC-modulation order and single-SB processing. The ambiguous BOC shape is also shown as a reference.

IV. THEORETICAL ANALYSIS

The goal is to estimate the optimal shift factor \hat{a} (shown in Fig. 4). For clarity of the theoretical derivation, we assume a static single-path channel model, where the Doppler shift has been already removed. The validity of the theoretical results has been also verified in multipath fading channels and for non-zero Doppler residual errors, via simulations. The received (modulated) signal $r(t)$ can be written as [12]:

$$r(t) = c(t) \otimes s_{BOC}(t) + \eta(t), \quad (2)$$

where $c(t) = \sum_{n=-\infty}^{\infty} (-1)^{nN_{BOC}} c_n \delta(t - nT_c)$ is the chip sequence, made of chips $\{c_n\}_n$, T_c is the chip interval, $\delta(\cdot)$ is the Dirac pulse, \otimes is the convolution operator, $s_{BOC}(t)$ is the BOC-modulation operator and $\eta(\cdot)$ is the additive white noise of the channel, of double-sided power spectral density σ_η^2 . We remark that, an additional factor $(-1)^{nN_{BOC}}$ is multiplied with the chip sequence in eq. (2), in order to take into account the odd BOC modulation orders, similar with [4], [21]. This means, that, in order to be able to model the sine and cosine BOC modulations in an unified format (for both even and odd BOC modulations, via eq. (3)), we need the above convention: for odd BOC-modulation orders, the chip sequence is first multiplied with an alternate sequence of +1s and -1s

and for even BOC modulation order, the chip sequence remains unchanged. This multiplication will not change the signal auto- and cross-correlation functions in a significant way, since the randomness of the code is still preserved after the chip inversion of every second bit.

In eq. (2), the continuous-time model was chosen for clarity of notations (but all the simulations are based on discrete-time model). In deriving the eq. (2), we used the Dirac function property that $\delta(t) \otimes x(t) = x(t)$, for any function $x(t)$. We also used the equivalent model of BOC-modulation waveform from [11], [12] which gives the expression of $s_{BOC}(t)$ in an unified form for SinBOC and CosBOC cases as:

$$s_{BOC}(t) = p_{T_B}(t) \otimes \sum_{i=0}^{N_{BOC}-1} \sum_{k=0}^{N_{cos}-1} (-1)^{i+k} \delta\left(t - i\frac{T_c}{N_{BOC}} - kT_B\right), \quad (3)$$

where $p_{T_B}(t)$ is a rectangular pulse of amplitude 1 for $t \in [0, T_B]$ (and 0 otherwise), N_{BOC} is the BOC-modulation order, N_{cos} is an index which tells us whether SinBOC or CosBOC modulation is used and which is equal to $N_{cos} = 1$ for SinBOC modulation and $N_{cos} = 2$ for CosBOC modulation [11], [12], and $T_B = \frac{T_c}{N_{BOC}N_{cos}}$ is the BOC sub-interval. The received signal can also be oversampled, with an oversampling factor N_s , which is assumed, for simplicity of the theoretical derivations to be 1 (however, this assumption is by no means compulsory, the analysis can be straightforwardly done with higher N_s as well).

The baseband reference PRN code $c_{ref}(t)$ of Fig. 4 is the BPSK-modulated PRN sequence, held at the same rate as the received signal, namely:

$$c_{ref}(t) = c(t) \otimes s_{BPSK,held}(t), \quad (4)$$

where $s_{BPSK,held}(t)$ is given by

$$s_{BPSK,held}(t) = p_{T_B}(t) \otimes \sum_{i=0}^{N_{hold}-1} \delta(t - iT_B). \quad (5)$$

Above, $N_{hold} = N_{BOC}N_{cos}N_s$ is the hold factor (needed in order to operate with input sequences of the same rate, as seen in Fig. 4).

The shifted received signal $r_s(t)$ of Fig. 6 is

$$r_s(t) = r(t)e^{\pm j2\pi f_c t a}, \quad (6)$$

where a is a shift parameter to be determined in what follows, and the received shifted signal after filtering $r_{filt}(t)$ can be written as:

$$r_{filt}(t) = r_s(t) \otimes g(t). \quad (7)$$

In eq. (6), the \pm sign stands for upper or lower shifting, respectively. In eq. (7), $g(t)$ is the impulse response of the SB selection filter (we do not expect the choice of the optimal parameter \hat{a} to be influenced by the filter design; this was verified by simulations, not reproduced here due to reasons of compactness).

Based on eqs. (2) to (7), the Power Spectral Density (PSD) $S_{\mathcal{R}}(f)$ at the output of the correlation $\mathcal{R}(t) = r_{filt} \otimes c_{ref}(t)$ can be therefore written (after straightforward manipulations) as:

$$S_{\mathcal{R}}(f) = \left(S_{PRN}(f \mp a f_c) |H_{BOC}(f \mp a f_c)|^2 |G(f \mp a f_c)|^2 + \sigma_{\eta}^2 \right) S_{PRN}^*(f) \left| H_{BPSK, held}(f) \right|^2 \quad (8)$$

where $*$ is the conjugate operator, $S_{PRN}(\cdot)$ is the PSD of the PRN code, which can be computed from its definition as:

$$S_{PRN}(f) = \sum_{n=-S_F+1}^{S_F-1} R_c(n) e^{-j2\pi n T_c t}, \quad (9)$$

$R_c(n) = \mathbf{E}(c_p c_{p+n}^*)$ is the code ACF, $\mathbf{E}(\cdot)$ is the expectation operator, $H_{BOC}(f)$ is the Fourier transform of the BOC-modulation operator given in eq. (3), and which can be brought in the following form after several manipulations (based on Fourier transform properties):

$$H_{BOC}(f) = T_B \text{sinc}(\pi f T_B) e^{-j\pi f T_B} \frac{1 - (-1)^{N_{cos}} e^{-j2\pi f T_c / N_{BOC}}}{1 + e^{-j2\pi f T_B}} \frac{1 - (-1)^{N_{BOC}} e^{-j2\pi f T_c}}{1 + e^{-j2\pi f T_c / N_{BOC}}}, \quad (10)$$

where $\text{sinc}(x) \triangleq \frac{\sin(x)}{x}$.

Furthermore, in eq. (8), $G(f)$ is the filter transfer function ($G(f)$ here was assumed to be a rectangular filter, either selecting only one main lobe, upper or lower, or selecting both main lobes and everything between them), and $H_{BPSK,held}(f)$ is the Fourier transform of the held BPSK waveform given in eq. (5), that is (for $N_s = 1$):

$$H_{BPSK,held}(f) = T_B \text{sinc}(\pi f T_B) e^{-j\pi f T_B} \frac{1 - e^{-j2\pi f T_c}}{1 - e^{-j2\pi f T_B}}. \quad (11)$$

The purpose of the unambiguous-BOC methods proposed in Fig. 4 is to maximize the correlation output at the correct delay, that is at zero timing lag, or equivalently, to maximize the area below the PSD $S_{\mathcal{R}}(f)$. It follows that the optimum shifting factor \hat{a} can be found as:

$$\hat{a} = \arg \max_a \mathcal{R}(0) = \arg \max_a \int_{B_T/2}^{B_T/2} S_{\mathcal{R}}(f) df. \quad (12)$$

where B_T is the bandwidth of the received signal (if infinite-bandwidth assumption is used, then $B_T = \infty$).

The solution of eq. (12) can be easily found numerically, after replacing $S_{\mathcal{R}}(f)$ with the values given in eqs. (8), (9), (10), and (11). We noticed via simulations that the noise variance σ_{η}^2 , the code properties (i.e., code type and spreading factor), and the method type (i.e., modified B&F, modified M&H and UAL) do not affect the optimal shift parameter. We have always obtained the same optimal shift factor \hat{a} , dependent only on the BOC-modulation order and on the type (i.e., SinBOC or CosBOC), as follows:

$$\hat{a} = \begin{cases} \frac{N_{BOC}}{2} & \text{if } N_{BOC} \text{ even, } \forall N_{cos} \text{ (i.e., both SinBOC and CosBOC)} \\ \frac{N_{BOC}-1}{2} & \text{if } N_{BOC} \text{ odd and SinBOC (i.e., } N_{cos} = 1) \\ \frac{N_{BOC}+1}{2} & \text{if } N_{BOC} \text{ odd and CosBOC (i.e., } N_{cos} = 2) \end{cases} \quad (13)$$

An example of the cost function (i.e., $\mathcal{R}(0)$) to be maximized is illustrated in Fig. 6 for an odd N_{BOC} order (i.e., $N_{BOC} = 3$), for two PRN codes (with different spreading factors, i.e., 1023 and 10230, respectively). We remark that the maximum is not achieved at $N_{BOC}/2$ (i.e., $a = 1.5$)

as expected from [15], [16], but rather at $\frac{N_{BOC}-1}{2}$ ($a = 1$), which justifies why the M&H method fails to work for odd BOC modulation orders. The same observation holds for the other proposed techniques (i.e., modified M&H and modified B&F methods).

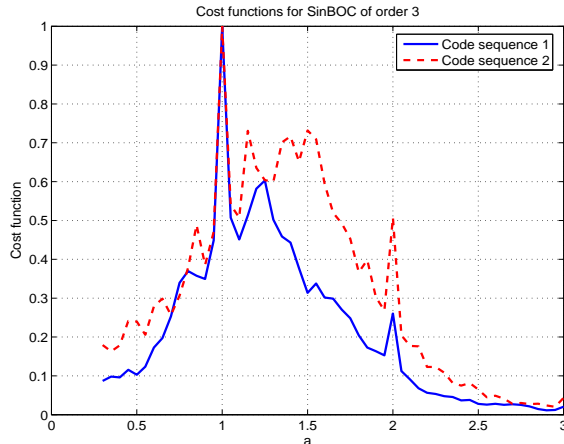


Fig. 6. Normalized cost function $\mathcal{R}(0)$ for UAL technique, SinBOC modulation, odd order $N_{BOC} = 3$ (the maximum here indicates the optimum shift parameter \hat{a}). Here, $\frac{N_{BOC}}{2}$ lies at $a = 1.5$ and $\frac{N_{BOC}-1}{2}$ lies at $a = 1$.

V. PERFORMANCE COMPARISON

The performance comparison is based on single-dwell serial-search acquisition and static channels [19], [22], where the step of searching the timing hypotheses $(\Delta t)_{bin}$ is taken equal to 0.5 chips, similar with [13]. The detection probability P_d is computed at a fixed false alarm probability $P_{fa} = 10^{-3}$ (i.e., the detection threshold is calculated adaptively, according to the Carrier-to-Noise Ratio (CNR) and to this fixed P_{fa}). The coherent N_c and non-coherent N_{nc} integration lengths are specified in the figures captions. The non-coherent integration time N_{nc} is given in units of blocks of code epochs of duration N_c . That is, if coherent integration of $N_c = 30$ ms is used, followed by $N_{nc} = 6$, the total integration time (coherent and non-coherent) is $30 \times 6 = 180$ ms. P_d depends on the sampling sequences, therefore uniform distribution of the sampling sequence (with respect to the channel delay) was assumed. Two detection probabilities are given: the average P_d

(obtained as an average over all possible sampling sequences) and the worst P_d (obtained for the worst sampling sequence with a step of 0.5 chips).

The average and worst detection probability curves are shown in Figs. 7, 8, 10 and 11, respectively. Figs. 7 and 8 are for odd BOC-modulation order, while Figs. 10 and 11 are for even BOC-modulation orders. The average detection probabilities are shown in Figs. 7 and 10, while the worst detection probabilities are shown in Figs. 8 and 11.

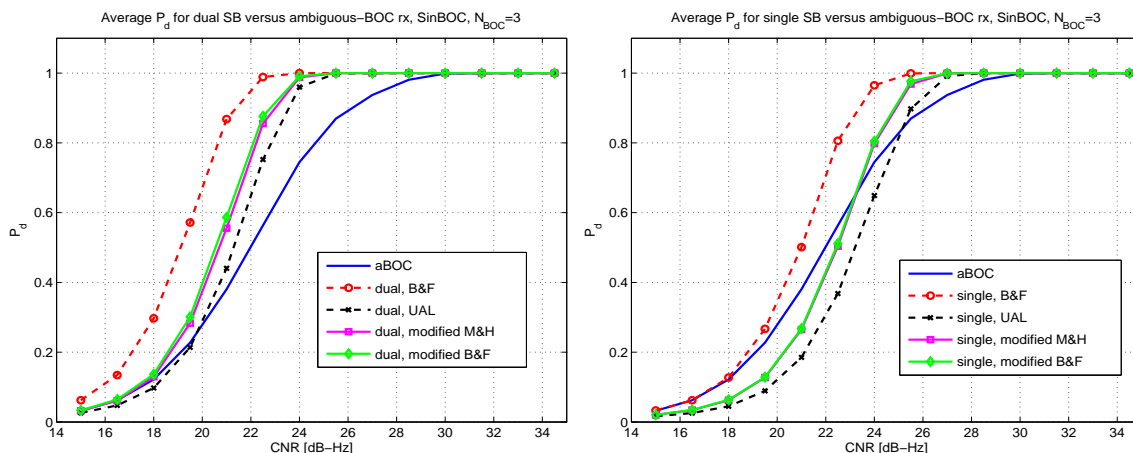


Fig. 7. Average detection probabilities for serial search, SinBOC modulation with odd N_{BOC} order: $N_{BOC} = 3$ (e.g., SinBOC(15,10)), $P_{fa} = 10^{-3}$, $N_c = 30$ ms, $N_{nc} = 6$. Left plot: dual-SB processing; right plot: single-SB processing.

The Mean Acquisition Times (MAT) based on the average detection probabilities for serial search are also shown in Fig. 9. It is assumed here that the full code length of 4092 chips is searched in one frequency bin. A penalty factor of 1 was used for the false alarm state. Obviously, since serial search is used in conjunction with long codes, the acquisition time is quite high. Hybrid or parallel search can be used to decrease MAT and is a topic of further investigation.

Similar plots have been obtained for other BOC-modulation orders (N_{BOC} values were varied between 2 and 14), with the observation that, for even N_{BOC} orders, we always obtained a better performance with unambiguous techniques than with **ambiguous-BOC (aBOC)** processing (similar with Fig. 10) for both SinBOC and CosBOC, and that the gaps between the unambiguous

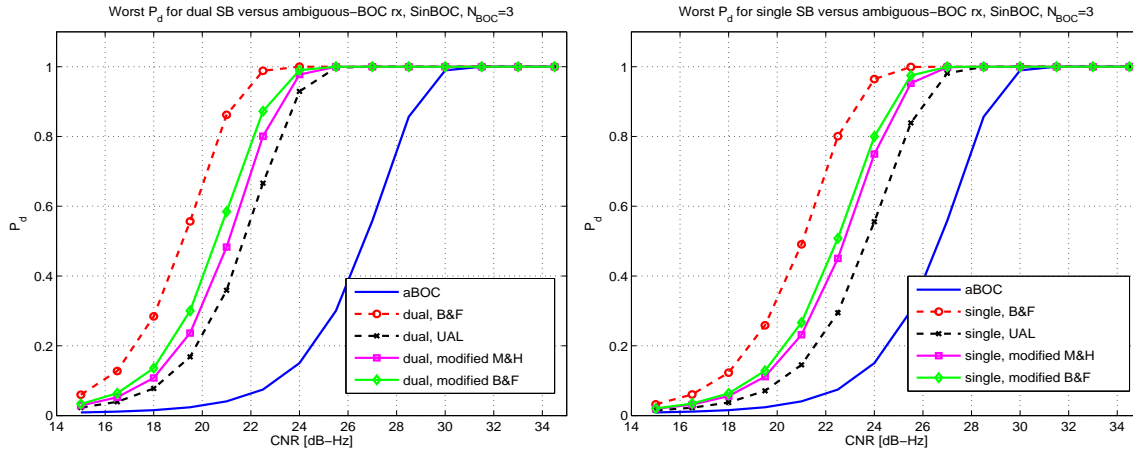


Fig. 8. Worst detection probabilities for SinBOC modulation with odd N_{BOC} order: $N_{BOC} = 3$ (e.g., SinBOC(15,10)), serial search, $P_{fa} = 10^{-3}$, $N_c = 30$ ms, $N_{nc} = 6$. Left plot: dual-SB processing; right plot: single-SB processing.

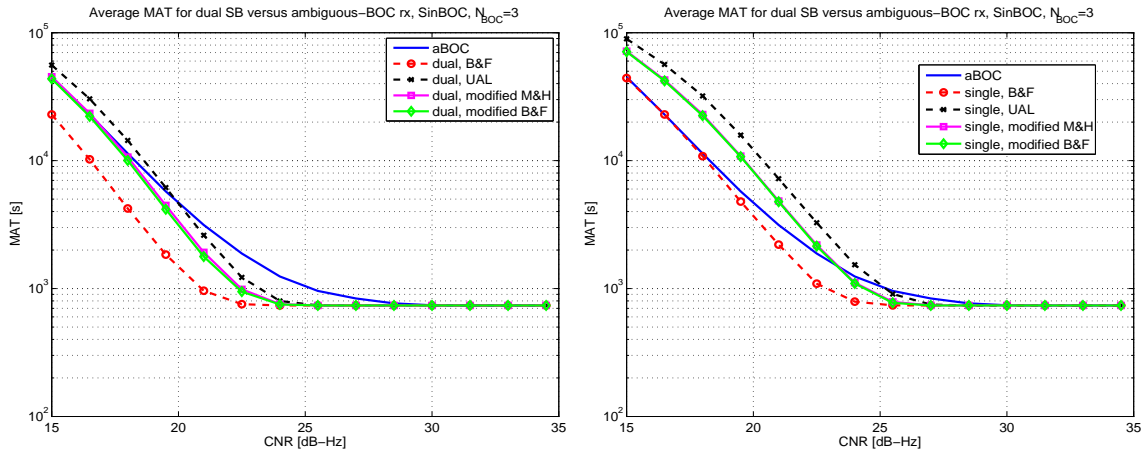


Fig. 9. Mean acquisition times for SinBOC modulation with odd N_{BOC} order: $N_{BOC} = 3$ (e.g., SinBOC(15,10)), serial search, single frequency bin, 4092-chip code length, $P_{fa} = 10^{-3}$, $N_c = 30$ ms, $N_{nc} = 6$. Left plot: dual-SB processing; right plot: single-SB processing.

processing techniques became smaller when N_{BOC} increased. This might be explained by the fact that, as N_{BOC} increases, the sidebands become more BPSK-like.

MAT based on the average detection probabilities for serial search and CosBOC modulation with even N_{BOC} order: $N_{BOC} = 12$ are also shown in Fig. 12.

We remark that the odd BOC-modulation orders give a poorer performance than the even

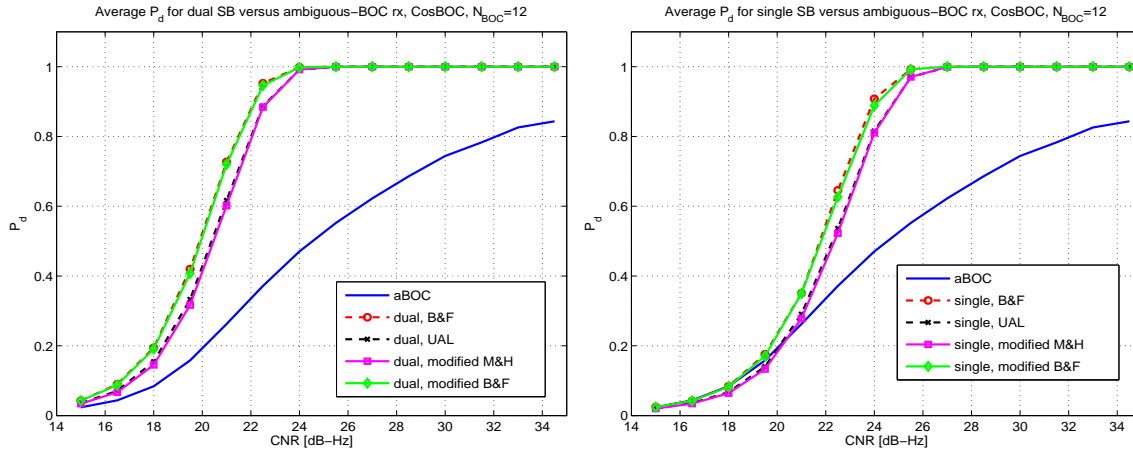


Fig. 10. Average detection probabilities for CosBOC modulation with even N_{BOC} order: $N_{BOC} = 12$ (e.g., CosBOC(15,2.5)), serial search, $P_{fa} = 10^{-3}$, $N_c = 30$ ms, $N_{nc} = 6$. Left plot: dual-SB processing; right plot: single-SB processing.

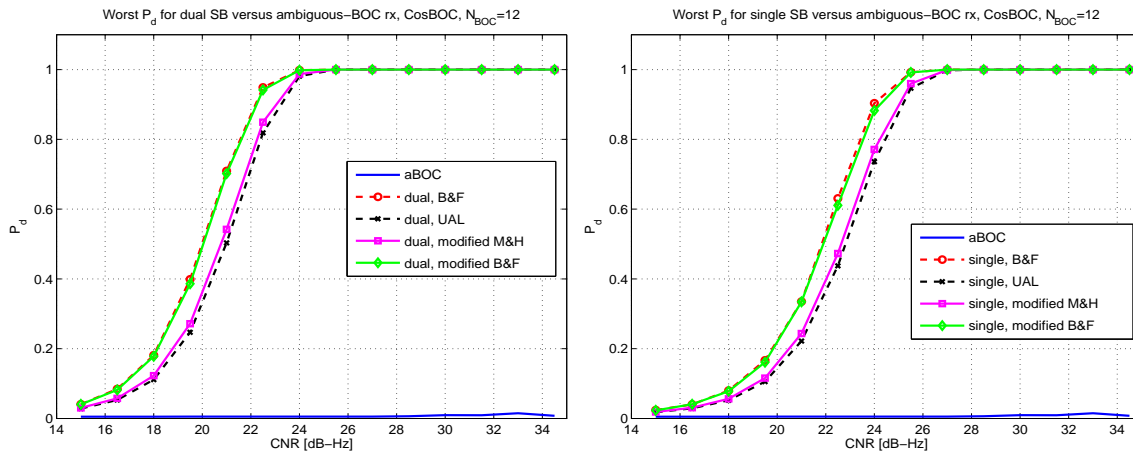


Fig. 11. Worst detection probabilities for CosBOC modulation with even N_{BOC} order: $N_{BOC} = 12$ (e.g., CosBOC(15,2.5)), serial search, $P_{fa} = 10^{-3}$, $N_c = 30$ ms, $N_{nc} = 6$. Left plot: dual-SB processing; right plot: single-SB processing.

BOC-modulation orders (for both SinBOC and CosBOC cases), which is mainly due to the fact that the zero-frequency content of odd BOC-modulation orders is quite significant, and, therefore, the spectrum of BOC signal is less similar to the spectrum of a BPSK signal shifted up and down around the sub-carrier frequency.

The P_d curves for M&H method were not drawn separately in Figs. 7 and 10, because they

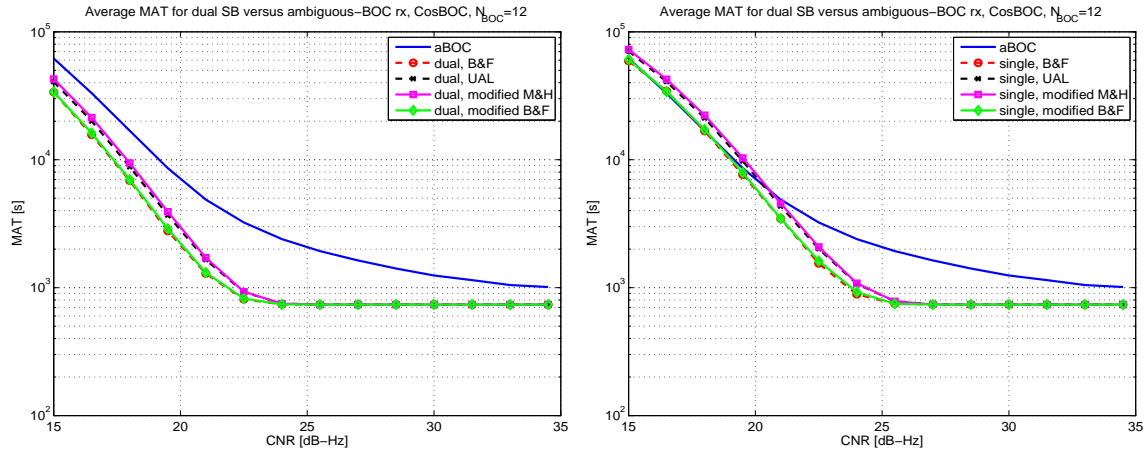


Fig. 12. Mean acquisition times for CosBOC modulation with even N_{BOC} order: $N_{BOC} = 12$ (e.g., Cos-BOC(15,2.5)), serial search, single frequency bin, 4092-chip code length, $P_{fa} = 10^{-3}$, $N_c = 30$ ms, $N_{nc} = 6$. Left plot: dual-SB processing; right plot: single-SB processing.

are perfectly overlapping with the curves for the modified M&H method if N_{BOC} is even, and they are close to P_{fa} level (i.e., close to zero), if N_{BOC} is odd (M&H method fails for odd N_{BOC} orders for reasons explained before).

We remark from Figs. 7 to 12 (and from the other simulations plots, not included here due to lack of space), that B&F method always gives the best performance among the unambiguous techniques, both for dual and single-SB processing. We also noticed that the performance deterioration (in terms of average P_d) when using one of the proposed methods compared with B&F method is between 0 and 2.5 dB, and it is higher for odd modulation orders and for dual SB processing than for even modulation orders or single-SB processing. We also remark that ambiguous BOC method fails to work for some sampling sequences and high BOC modulation orders, as seen in Fig. 11. This is due to the step of 0.5 chips which is used here, and which is not enough to capture the main lobe of the ACF. It can be also seen from Figs. 7 to 12 that there is a significant improvement of the unambiguous BOC methods over the ambiguous methods, especially if a bad sampling sequence were to occur (see the plots for worst P_d case).

The UAL method, which will be shown in Section VI to be the least complex, gave the poorest

performance among the considered unambiguous methods, but the differences are only up to 1.5 dB (the gap is smaller than 1 dB when N_{BOC} is even). Moreover, UAL performance (from the point of view of the average P_d) is still much better than that of ambiguous-BOC processing if N_{BOC} is even. For odd N_{BOC} and average P_d , the unambiguous processing is not always better than the ambiguous processing: the CNR should be high enough in order to have some significant gain of unambiguous BOC processing versus ambiguous BOC processing. From the worst P_d point of view, UAL always outperforms the ambiguous BOC.

VI. COMPLEXITY CONSIDERATIONS

The complexity of the acquisition structures depends, on one hand, on the filtering part, and, on the other hand, on the correlation part.

The correlations can be implemented either in time domain, or in frequency domain [20]. For frequency-based correlation, all the considered methods have similar requirements (in terms of additions and multiplications), and the only difference will come from the filtering part. For time-domain correlation, if the reference code is kept at ± 1 level, a reduced-complexity correlation method has been described in [20]. On the other hand, if the reference code is complex-valued, as it is the case for B&F and M&H methods, there is only the so-called direct approach, whose complexity (in terms of additions and multiplications) has been derived in [20].

To recall the results from [20], the number of real additions N_{adds} required for the reduced-complexity correlation method (i.e., when the reference code is a sequence of ± 1 such as in our proposed approaches), per each frequency bin and for single SB processing³, is equal to:

³ For dual SB processing, the number of computations is doubled.

$$\begin{aligned}
N_{adds} = & 2N_{nc} \left(\left(N_{\tau}(N_c S_F - 1) + N_s N_{BOC} - 1 \right) \left(N_s N_{BOC} D_{max} / N_{\tau} - 1 \right) \right. \\
& \left. + N_s N_{BOC} (N_c S_F - 1) \right) \quad (14)
\end{aligned}$$

and there are no multiplications involved here (only additions and sign inversions, due to the particular structure of the reference code). Above, N_{nc} is the non-coherent integration length (in blocks of code epochs), N_c is the coherent integration length (in ms), N_s is the oversampling factor (or the number of samples per BOC interval), N_{τ} is the step of searching the timing hypotheses, expressed in samples (i.e., $N_{\tau} = N_s N_{BOC} (\Delta t)_{bin}$ for SinBOC modulation and $N_{\tau} = 2N_s N_{BOC} (\Delta t)_{bin}$ for CosBOC modulation), S_F is the PRN code spreading factor (or the code epoch length), and D_{max} is the maximum delay search range, expressed in chips (e.g., for full search, $D_{max} = S_F$).

On the other hand, when the direct approach has to be used to compute the correlations (such as in B&F and M&H methods, where the correlation is done with a complex reference sequence, see Figs. 1 and 2), we have the following number of real additions and multiplications [20]:

$$N_{adds, \text{direct-form}} = 2N_{nc} \left(3N_c S_F N_s N_{BOC} - 1 \right) N_s N_{BOC} D_{max} / N_{\tau}, \quad (15)$$

and, respectively:

$$N_{mults} = 4N_{nc} (N_c S_F N_s N_{BOC}) \frac{N_s N_{BOC} D_{max}}{N_{\tau}}. \quad (16)$$

Based on eqs. (14) to (16) and on the discussion above, the number of required filters and required additions and multiplications (for a time-based correlation) are shown in Tables I and II, respectively, for all the considered methods. The term N_{sh} is due to the shifting with the exponential term $\exp(\pm j2\pi\hat{a}f_c t)$, where \hat{a} is the shift factor and f_c is the chip rate, and it is obviously much smaller than N_{adds} and N_{mults} , especially when D_{max} is high:

$$N_{sh} = N_s N_{BOC} S_F N_c N_{nc} \quad (17)$$

The shifting is applied at sample level, and for both in-phase and quadrature components of the received signal (different shifting factor for upper and lower sidebands). The shifting complexity can be reduced if the sampling frequency is an integer multiple of chip rate, but we concentrate here on general case. Moreover, a receiver generally has a sampling frequency which is asynchronous to the chip rate [23]. Also, generating sinusoid waveforms for the shifting part may add additional complexity. This is considered to be rather small compared with the other factors and it is not taken into account here. Alternatively, the sine waveform generation is not necessary implemented as an additional block, as the shifting can be performed as a part of the already existing carrier phase rotation.

The number of required additions and multiplications for frequency-based correlation are not shown here since they are the same for all the methods⁴ and since the main interest here is on low-complexity time-domain implementations. The front-end filtering, which is assumed to be the same for all the considered methods, was not included in the filter count of Table I.

We remark that the following rules have been used in computing the values of Table I: one complex filter applied to a complex signal is equivalent to 4 real filters. One real filter applied to a complex signal or one complex filter applied to a real signal is equivalent to 2 real filters. The filter is real if it has even symmetry (in amplitude response) and odd symmetry (in phase response) with respect to the 0 frequency.

We remark from Tables I and II and from the results reported in Section V, that there is a tradeoff between the complexity of the acquisition unit and the algorithm performance. The values for the number of required additions have been computed based on eqs. (14) and (15), by assuming a step of the time bin of $(\Delta t)_{bin} = 0.5$ chips. Independently of the other parameters, for this time-bin step, the simulation results showed that $N_{adds,direct-form}$ is about 6 times higher than N_{adds} .

⁴ Their exact expression can be found in [20].

⁵ N_{adds} is given by eq. (14) and N_{sh} by eq. (17).

TABLE I

NUMBER OF FILTERS AND LIMITS FOR THE AMBIGUOUS AND UNAMBIGUOUS ACQUISITION TECHNIQUES (THE PROPOSED METHODS ARE WITH BOLDFACED LETTERS).

Method	Number of real filters needed		Limits of method
	dual	single	both dual/single
B&F	12	6	works for $\forall N_{BOC}$
M&H	2	2	does not work for N_{BOC} odd
modified M&H	8	4	works for $\forall N_{BOC}$
modified B&F	8	4	works for $\forall N_{BOC}$
UAL	0	0	works for $\forall N_{BOC}$
aBOC	0	0	works for $\forall N_{BOC}$

TABLE II

COMPUTATIONAL COMPLEXITY OF CORRELATION PART FOR THE AMBIGUOUS AND UNAMBIGUOUS ACQUISITION TECHNIQUES (THE PROPOSED METHODS ARE WITH BOLDFACED LETTERS). $(\Delta t)_{bin} = 0.5$ CHIPS.

Method	Required additions for time-based correlation stage ⁵ , $N_{sh} \ll N_{adds}$		Required multiplications for time-based correlation stage ⁶ , $N_{sh} \ll N_{muls}$	
	dual	single	dual	single
B&F	$\approx 12N_{adds}$	$\approx 6N_{adds}$	$2N_{muls}$	N_{muls}
M&H	$\approx 6N_{adds} + 6N_{sh}$	$\approx 6N_{adds} + 3N_{sh}$	$2N_{muls} + 4N_{sh}$	$N_{muls} + 4N_{sh}$
modified M&H	$2N_{adds} + 6N_{sh}$	$N_{adds} + 3N_{sh}$	$4N_{sh}$	$4N_{sh}$
modified B&F	$2N_{adds} + 6N_{sh}$	$N_{adds} + 3N_{sh}$	$4N_{sh}$	$4N_{sh}$
UAL	$2N_{adds} + 6N_{sh}$	$N_{adds} + 3N_{sh}$	$4N_{sh}$	$4N_{sh}$
aBOC	N_{adds}		0	

For a comparison between the number of operations required by different methods, we also selected several typical filter implementations with Finite-Impulse-Response (FIR) or Infinite-Impulse-Response (IIR) [24], [25], [26], as shown in Table III. Table III does not give an exhaustive description of possible filters structures, but rather some estimates about the expected complexity of the filtering part. The filter orders are denoted via N_{FIR} and N_{IIR} , respectively, and they are parameters of the design process. Comparing some numerical values of the complexity in

⁶ N_{muls} is given by eq. (16).

TABLE III
 FILTERS COMPLEXITY (I.E., NUMBER OF OPERATIONS FOR 1 MS RECEIVER PROCESSING) PER REAL FILTER FOR
 DIFFERENT FILTERING STRUCTURES.

Operation	FIR symmetrical [24]	IIR Direct form [25]	IIR Lattice [25]	IIR Lossless discrete integrators [26]
Multiplications	$\lceil \frac{N_{FIR}}{2} \rceil \cdot N_{sh}$	$(2N_{IIR} + 1) \cdot N_{sh}$	$N_{IIR} \cdot N_{sh}$	$N_{IIR} \cdot N_{sh}$
Additions	$(N_{FIR} - 1) \cdot N_{sh}$	$2N_{IIR} \cdot N_{sh}$	$3N_{IIR} \cdot N_{sh}$	$2N_{IIR} \cdot N_{sh}$

the filtering and correlation parts we noticed that the main complexity comes from the correlation part.

The total number of operations (additions plus multiplications) is shown for illustration in Fig. 13, for SinBOC(1,1) modulation, 1 ms processing (i.e., $N_c = 1$ ms, $N_{nc} = 1$), single frequency bin and $S_F = 4092$ chips [9]. In the left plot of Fig. 13, the maximum delay spread is varied from few chips (assisted acquisition) to full code search ($D_{max} = S_F$), while oversampling factor is kept to the minimum $N_s = 1$. In the right plot of Fig. 13, N_s is varied, while $D_{max} = S_F$ (non-assisted acquisition). The step of scanning the time bins is $(\Delta t)_{bin} = 0.5$ chips. The filter considered here was an IIR discrete lossless integrator with filter order $N_{IIR} = 3$; however, the results are not affected significantly if the other filter types considered in Table III are employed.

Based on Figs. 7, 10 and 13, we see that the dual B&F method has the best performance, but also the highest complexity. The complexity of the M&H method is also quite close to that of the B&F method (only slightly smaller). All three proposed methods provide a significant decrease in complexity, similar to the ambiguous BOC technique (but the performance of the unambiguous techniques is typically much better than that of aBOC technique, as it was shown in Section V). The greater the maximum delay search range is, the greater the gap between the proposed methods' complexity and the existing methods' complexity. Modified M&H and modified B&F methods have the same complexity, therefore the modified B&F method is to be preferred between the two, since it gives slightly better performance. The tremendous reduction in complexity of the proposed

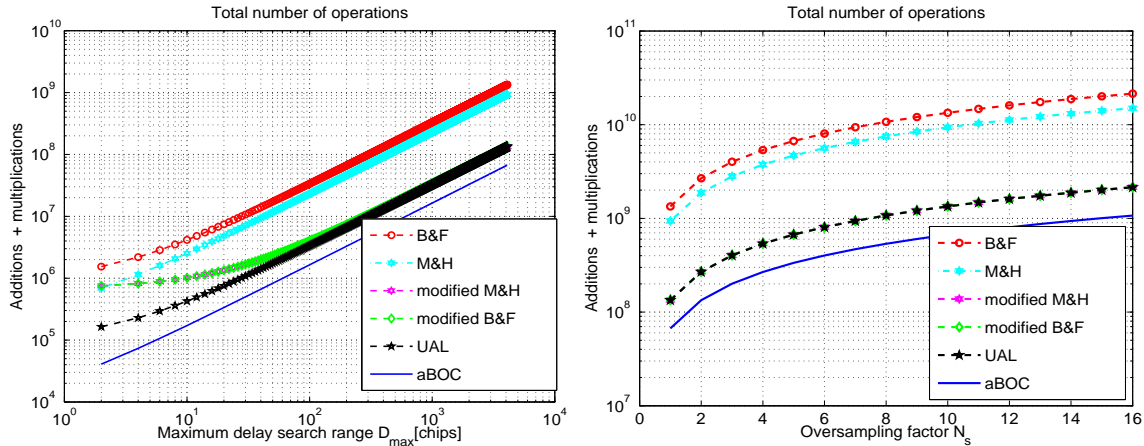


Fig. 13. Example of required additions and multiplications for unambiguous processing compared with ambiguous BOC processing. SinBOC(1,1). Left: variation with respect to the delay search range. Right: variation with the oversampling factor. The curves are overlaid (i.e. identical) for modified M&H and modified B&F on left plot, and for UAL, modified M&H, and modified B&F on right plot.

methods is valid for both assisted and non-assisted acquisition (left plot of Fig. 13) and for any oversampling factor (right plot of Fig. 13).

Based on the performance and complexity plots, we conclude that, if N_{BOC} is sufficiently high, then the best tradeoff between performance and complexity is given by the proposed single-SB UAL method (e.g., for $N_{BOC} = 12$, the performance of single-SB UAL method is very close to the performance of the B&F method, as seen in Fig. 10). For lower N_{BOC} orders, the modified B&F approach (both single and dual) has a performance similar to the performance of B&F method (especially for even N_{BOC}) while its implementational complexity is significantly lower.

VII. CONCLUSIONS

Our paper introduced three low-complexity methods which removed the ambiguities in the envelope of the ACF of a split-spectrum signal. The most important application of our methods lies within Galileo and modernized GPS signals, where sine and cosine BOC-modulation types have been selected as the main candidates for the transmission of the PRN codes. However, the theoretical derivations presented in Section IV may find their applicability in other classes of split-

spectrum CDMA signals.

We showed that the existing unambiguous BOC acquisition techniques, while decreasing the computational load compared with the ambiguous-BOC-acquisition method, still suffer of high complexity of implementation, and some of them are unable to cope with odd BOC-modulation orders. We introduced a new theoretical framework based on the power spectral densities of the received signals, which allows us to choose, in an optimal way, the parameters of an unambiguous-BOC-acquisition method, such that both even and odd BOC-modulation orders are covered. Moreover, the unambiguous techniques (existing and proposed) have been compared for cosine BOC-modulation cases, as well as for odd BOC-modulation orders.

We presented both the performance curves (i.e., detection probabilities) and estimates of the algorithmic complexity for the proposed methods and we compared them with the existing ones. Both the filtering part and the correlation part were taken into account when studying the algorithmic complexity. Further optimization on filter design is still possible, such as joint design of sideband selection filter and receiver front-end filtering, or inter-changing the places of the shifting unit with the filtering unit [27]. However, the computational gain of the proposed methods comes mainly from the correlation part, hence, it is expected that they will keep this advantage over the other unambiguous acquisition methods even if the filter structures are optimized. The main trade-off when choosing one of the analyzed unambiguous methods is between the desired performance and the targeted complexity. The lowest complexity unambiguous method proposed here is the Unsuppressed Adjacent Lobes UAL method, which also provides very good performance (not far from the performance of B&F method) for the even-order BOC modulations that are the main candidates for the future satellite navigation signals.

REFERENCES

- [1] J. H. Reed, K. J. Krizman, B. D. Woerner, and T. S. Rappaport, "An overview of the challenges and progress in meeting the E-911 requirement for location service," *IEEE Communications Magazine*, vol. 36, pp. 30–37, Apr 1998.
- [2] G. Heinrichs, R. Bischoff, and T. Hesse, "Receiver architecture synergies between future GPS/Galileo and UMTS/IMT-2000," in *Proc. of IEEE 56th Vehicular Technology Conf. (VTC) Fall*, pp. 1602–1606, 2002.
- [3] M. Quinlan, G. Burden, S. Rollet, R. D. Gaudenzi, and S. Harding, "Validation of novel navigation signal structures for future GNSS systems," in *Proc. of IEEE Position Location and Navigation Symposium (PLANS)*, pp. 389–398, Apr 2004.
- [4] J. Betz, "The Offset Carrier Modulation for GPS modernization," in *Proc. of ION Technical meeting*, (Cambridge, Massachusetts), pp. 639–648, Jun 1999.
- [5] B. Barker, J. Betz, J. Clark, J. Correia, J. Gillis, S. Lazar, K. Rehorn, and J. Straton, "Overview of the GPS M Code Signal," in *CDROM Proc. of NMT*, 2000.
- [6] G. Hein, J. Godet, J. Issler, J. Martin, T. Pratt, and R. Lucas, "Status of Galileo frequency and signal design," in *CDROM Proc. of ION GPS*, (Portland, Oregon), Sep 2002.
- [7] G. Hein, M. Irsigler, J. A. Rodriguez, and T. Pany, "Performance of Galileo L1 signal candidates," in *CDROM Proc. of European Navigation Conference GNSS*, May 2004.
- [8] L. Ries, F. Legrand, L. Lestarquit, W. Vigneau, and J. Issler, "Tracking and multipath performance assessments of BOC signals using a bit-level signal processing simulator," in *Proc. of ION-GPS2003*, (Portland, OR, US), pp. 1996–2009, Sep 2003.
- [9] GJU, "Galileo standardisation document for 3GPP." Galileo Joint Undertaking (GJU) webpages, <http://www.galileoju.com> (active May 2006), May 2005.
- [10] S. H. Raghavan and J. K. Holmes, "Modeling and simulation of mixed modulation formats for

- improved CDMA bandwidth efficiency,” in *Proc. of Vehicular Technology Conference*, vol. 6, pp. 4290–4295, Sep 2004.
- [11] E. S. Lohan, A. Lakhzouri, and M. Renfors, “Spectral shaping of Galileo signals in the presence of frequency offsets and multipath channels,” in *CDROM Proc. of IST Mobile & Wireless Communications Summit*, (Dresden, Germany), Jun 2005.
- [12] E. S. Lohan, A. Lakhzouri, and M. Renfors, “Binary-Offset-Carrier modulation techniques with applications in satellite navigation systems.” *Wiley International Journal of Wireless Communications and Mobile Computing*, DOI: 10.1002/wcm.407, published on-line, Jul 2006.
- [13] P. Fishman and J. Betz, “Predicting performance of direct acquisition for the M-code signal,” in *Proc. of ION NMT*, pp. 574–582, 2000.
- [14] J. Betz and B. Titus, “Intersystem and intrasystem interference with signal imperfections.” MITRE Technical Papers, www.mitre.org/work/tech_papers/ (active May 2006), Jan 2004.
- [15] N. Martin, V. Leblond, G. Guillotel, and V. Heiries, “BOC(x,y) signal acquisition techniques and performances,” in *Proc. of ION-GPS2003*, (Portland, OR, US), pp. 188–198, Sep 2003.
- [16] V. Heiries, D. Oviras, L. Ries, and V. Calmettes, “Analysis of non ambiguous BOC signal acquisition performance,” in *CDROM Proc. of ION GNSS*, (Long Beach, CA), Sep 2004.
- [17] J. Betz and P. Capozza, “System for direct acquisition of received signals.” US Patent Application Publication 2004/0071200 A1, Apr 2004.
- [18] S. Fischer, A. Guerin, and S. Berberich, “Acquisition concepts for Galileo BOC(2,2) signals in consideration of hardware limitations,” in *Proc. of IEEE Vehicular Technology Conference*, vol. 5, pp. 2852–2856, May 2004.
- [19] E. S. Lohan, “Statistical analysis of BPSK-like techniques for the acquisition of Galileo signals,” in *CDROM Proc. of 23rd AIAA/IEEE International conference on Communications and*

satellite Systems (ICSSC), (Rome, Italy), Sep 2005.

- [20] A. Lakhzouri, E. S. Lohan, and M. Renfors, “Reduced-Complexity Time-Domain Correlation for Acquisition and Tracking of BOC-Modulated Signals,” in *CDROM Proc. of ESA-NAVITEC*, Dec 2004.
- [21] E. Rebeyrol, C. Macabiau, L. Lestarquit, L. Ries, and J. L. Issler, “BOC power spectrum densities,” in *CDROM Proc. of ION-NMT*, (San Diego, CA), Jan 2005.
- [22] A. Lakhzouri, E. S. Lohan, and M. Renfors, “Hybrid-search single and double-dwell acquisition architectures for Galileo signal,” in *CDROM Proc. of IST mobile & wireless communications summit*, Jun 2004.
- [23] W. D. Wilde, J.-M. Sleewaegen, K. V. Wassenhove, and F. Wilms, “A First-of-a-Kind Galileo Receiver Breadboard to Demonstrate Galileo Tracking Algorithms and Performances,” in *ION GNSS*, Sep 2004.
- [24] J. Z. Mou, “Minimal structures for symmetric FIR filters of arbitrary length,” *IEEE Transactions on Signal Processing*, vol. 41, pp. 1790–1808, 1993.
- [25] J. Yli-Kaakinen, *Optimization of digital filters for practical implementations*. PhD thesis, Tampere University of Technology, Jun 2002.
- [26] F. Balestro, A. Chianale, G. Privat, M. Tawfik, T. Vandeweerd, and A. D. Wittmann, “Design of digital filters for advanced telecommunications ASIC’s using a special-purpose silicon compiler,” *IEEE Journal of Solid-State Circuits*, vol. 26, pp. 1047–1055, Jul 1991.
- [27] A. Burian, E. S. Lohan, V. Lehtinen, and M. Renfors, “Complexity considerations for unambiguous acquisition of Galileo signals,” in *Proc. of the Workshop on Positioning, Navigation and Communication (WPNC)*, (Hannover, Germany), pp. 65–73, 2006.